Nova Science Publishers, Inc. Hauppauge, New York
Journal of Nature Science and Sustainable Technology, Volume 2, Issue 3, 2007
ISSN 1933-0324

ROCK AND FLUID TEMPERATURE CHANGES DURING THERMAL OPERATION IN EOR PROCESS

M Enamul Hossain
S Hossein Mousavizadegan
M Rafiqul Islam
Dalhousie University

ABSTRACT

The temperature distribution in a reservoir formation is becoming a very important issue due to its utilization in detecting water or gas influx or type of fluid entering into the wellbore. This information is necessary for better reservoir management. Prediction of temperature distribution behavior during the steam injection or thermal process is significant for production evaluation of field operations. Such a prediction can be used in the case of hot water injection into a reservoir and also applies in some other thermal recovery processes, such as in-situ combustion. This study investigated temperature propagation pattern and its dependence on various parameters during steam flooding. The model equation has been solved for temperature distribution throughout the reservoir for different cases. It is found that the fluid and rock matrix temperature difference is negligible. Results show that formation fluid velocity, steam injection velocity, and time have an impact on temperature profiles behavior.

INTRODUCTION

Steam flooding is a process whereby steam is injected into a number of wells while the oil is produced from adjacent wells (Figure 1). For generating steam or hot water, solar energy can be used for sustainability with a direct solar heating system. This direct solar heating technique has been demonstrated by Hossain (Kays et al., 1982; Chu, 1983; Khan et al., 2005; Hossain et al., 2008). In some steam flooding operations, the produced gas has some residual heating value that can be utilized to heat the water. This heat can also be used to preheat the water. The flue gas passes through a small furnace to burn before releasing into atmosphere. Finally, the chemical heat energy and furnace heat is used to preheat the water. This process not only lowers the steam generation cost but also reduces the amount of air pollutants released into the surrounding. This process will improve lower the costs of the steam flooding process while reducing environmental pollution.

The temperature distribution is very important in thermal oil recovery. Increasing the temperature in the formation, the mobility of heavy viscous fluid increases the levels of oil

that is produced. As the steam moves away from the well, its temperature drops as it continues to expand in response to pressure drop. At some distance from the well, the steam starts to condense and forms a hot water zone. In the steam zone, the oil is displaced by gas (steam) drive. In the hot water zone, physical changes in the characteristics of oil and reservoir rock take place and result in additional oil recovery.

The understanding of temperature propagation through a formation is important in the design of thermal injection projects. Temperature profile may be used to predict the fracture characteristics in the reservoir. It can be applied to identify water or gas entries in the reservoir. It is also important to guide the action of sliding sleeves or other downhole flow control devices. Therefore, it is useful to investigate the pattern of temperature propagation and heat exchange between fluid and rock in the formation.

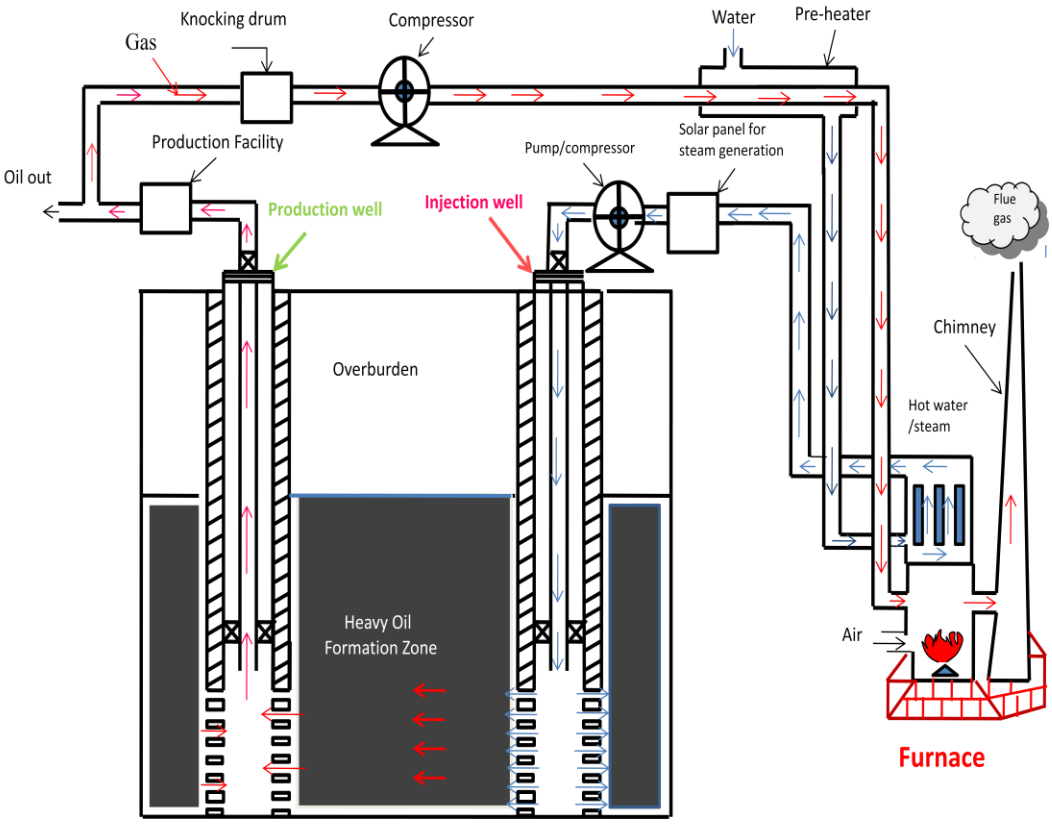

Figure 1. Mechanism of Oil recovery scheme using injection and production wells in an oil field reservoir

The properties of fluid and matrix are functions of the media temperature and pressure. So, it is necessary to know the temperature and pressure distribution to predict these properties. When rock and fluid temperature are different in the formation, it behaves like hydraulic fracture flow in the formation. Atkinson and Ramey (1977) presented mathematical models to study heat transfer behavior in fractured and non-fractured porous media. The models are used to calculate the temperature distributions caused by nonisothermal fluid flow through a uniform porous medium. They concluded that their models are useful to find the relative importance of different heat transfer mechanisms. They assumed a uniform and

constant fluid flow in the formation. They also considered a uniform temperature in the reservoir for both fluid and rock matrix. They neglected the heat transfer in the solid rock matrix.

Crookston et al. (1979) presented a model for numerically simulating thermal recovery processes. The simulator describes the flow of water, oil, and gas. They showed the temperature distribution with time. They include gravity and capillary effects but did not include the effects of formation fluid velocity and injection steam velocity. They showed heat transfer by conduction, convection, and vaporization condensation of both water and hydrocarbons. However, they discarded the effects of the rock and fluid temperature difference. Meyer (1989) proposed a combined convection along a vertical fracture with conduction and convection in the reservoir. He investigated temperature distribution throughout the reservoir for both fracture and non-fracture conditions by varying different heat rates. He took into account that the rock and fluid temperatures are the same. He did not study the different parameters that may affect temperature distribution.

Akin (2004) proposed a mathematical model for gravity drainage in heavy oil reservoirs and tar sands during steam injection. In his model, he assumed a temperature profile which is only time-dependent and decline exponentially with distance from the interface. However, he acknowledged that with the increase of steam temperature, oil rate increases. He did not validate this argument and did not consider other influential factors such as liquid velocity, steam velocity, and temperature difference between rock and fluid. Cheng and Kuznetsov (2005) studied heat transfer in a helical pipe filled with a fluid saturated porous medium. They investigated the effects of the Darcy number, the Forchheimer coefficient, Dean and Germano numbers on the axial flow velocity, secondary flow, temperature distribution, and the Nusselt number. Their numerical simulations of heat transfer in the media was based on laminar flow of a Newtonian fluid in a helical pipe filled with a fluid saturated porous medium subjected to a constant wall heat flux. They did not study the effects of fluid velocity on rock and fluid temperature distribution. Yoshioka et al. (2005) presented a model for predicting the temperature profile in a horizontal well. This is for a steady state flow condition. They assumed the reservoir is ideally isolated with each segment. They considered a box-shaped homogeneous reservoir. They investigated the effects of production rate, permeability and fluid types on temperature profiles. However, they did not investigate the effects of formation fluid and steam injection velocity.

Dawkrajai et al. (2006) studied the water entry location identification by temperature profile in a horizontal well. They varied the production rate and types of oil to see their effects on temperature profile. They assumed that flowing fluid and rock temperature are the same. They did not check the effects of fluid velocity and injection steam velocity on temperature distribution. Jiang and Lu (2006) investigated fluid flow and convective heat transfer of water in sintered bronze porous plate channels. The numerical simulations assumed a simple cubic structure with homogeneous particles. They also considered a small contact area and a finite-thickness wall subject to a constant heat flux at the surface. They numerically determined some fluid and rock properties. They also studied temperature distributions in the porous media. They only nominally investigated the effects of fluid velocity on temperature distribution. They recommended further investigations of the boundary characteristics and internal phenomena controlling heat transfer in porous media. In

the present study, these criteria have been investigated to find the role of these parameters in temperature distribution throughout the reservoir.

Hossain et al. (2007) investigated temperature propagation pattern and its dependence on various parameters during thermal flooding. The model equation has been solved for temperature distribution throughout the reservoir for different cases. Results show that formation fluid velocity and time have an impact on temperature profiles behavior. They also showed that temperature distribution is much more sensitive to time, and formation fluid velocity. However, they did not investigate the effects of hot water injection rate or velocity. It is known that temperature profile is sensitive to steam or hot water injection rate or velocity. The shape and type of the temperature profile is dependent on fluid and steam velocity.

Significant work has been done on fluid property changes due to heat loss in the reservoir formation. It is due to the more tempting changes of fluid properties with temperature change. However, there is little in the literature that deals with temperature propagation in the formation. The effects of formation fluid velocity and steam velocity on temperature distribution are still ignored by the researchers. There is no existing literature that investigates the effects of fluid and rock temperature separately. This study investigates these aspects.

THEORITICAL DEVELOPMENT

To determine temperature distribution with space and time, energy balance equation is considered to be the governing equation for both rock and fluid separately. The partial differential equations have a familiar form because the system has been averaged over representative elementary volumes (REV). A right handed Cartesian coordinate system is considered where the *x*-axis is along the formation length. The general form of differential energy balance equations in three dimensions may be given as (Chan and Banerjee, 1981; Kaviany, 2002)

$$\nabla\left(k_s \times \nabla T_S\right) = \left(1-\phi\right)\left(\rho c_p\right)_s \frac{\partial T_s}{\partial t} + h_c\left(T_s - T_f\right) \tag{1}$$

$$\nabla\left(k_f \times \nabla T_f\right) - \left(\rho\, c_p\right)_f \left(\nabla \bar{V}\right) T_f = \phi\left(\rho\, c_p\right)_f \frac{\partial T_f}{\partial t} + h_c\left(T_f - T_s\right) \tag{2}$$

where T_s and T_f are the rock matrix and fluid temperatures, respectively. These represent the thermal state of each phase in the same REV.

It takes into account a porous medium of uniform cross sectional area homogeneous along the *x*-axis. It is normal practice to consider that the fluid flow in porous media is governed by Darcy's law. It is also considered that the thermal conductivity of the fluid and solid rock matrix is not a function of temperature and is constant along the media. Therefore, equations (1) and (2) can be written in one dimensional form as

$$k_S \frac{\partial^2 T_s}{\partial x^2} = (1-\phi)\rho_s c_{ps} \frac{\partial T_s}{\partial t} + h_c (T_s - T_f) \tag{3}$$

$$k_f \frac{\partial^2 T_f}{\partial x^2} - \rho_f c_{pf} u \frac{\partial T_f}{\partial x} = \phi \rho_f c_{pf} \frac{\partial T_f}{\partial t} + h_c (T_f - T_s) \tag{4}$$

where,

$$\rho_f c_{pf} = \rho_w c_{pw} S_w + \rho_o c_{po} S_o + \rho_g c_{pg} S_g \tag{5}$$

$$k_f = k_w + k_o + k_g \tag{6}$$

$$\rho_f = \rho_w S_w + \rho_o S_o + \rho_g S_g \tag{7}$$

$$S_w + S_o + S_g = 1 \, . \tag{8}$$

The length of the heated region can be estimated using a model developed by Marx and Langenheim (1959). The amount of energy required to increase the temperature of a porous rock is easily calculated from thermodynamic tables and heat capacity data at constant pressure. If we consider a constant rate of heat generation per unit volume Q_g is maintained then equation (9) gives total energy required to increase the temperature of *1 ft*^{3} of reservoir rock from an initial temperature, T_s to a higher temperature, T_{hs} (in ^{0}F) (Green and Willhite, 1998).

$$Q_g = M(T_{hs} - T_s) \tag{9}$$

where, $M = (1-\phi)\rho_s c_{ps} + \phi S_o \rho_o c_{po} + \phi S_w \rho_w c_{pw} + \phi S_g \rho_g c_{pg}$ (10)

The mean heat capacities of each component are based on the temperature difference. It can be defined as (Green and Willhite, 1998):

$$\begin{aligned} &c_{pw} = (H_{wTf} - H_{wr}) / (T_f - T), \; c_{po} = (H_{oTf} - H_{oTi}) / (T_f - T_i), \\ &c_{ps} = (H_{sTf} - H_{sTi}) / (T_f - T), \; c_{pg} = (H_{gTf} - H_{gTr}) / (T_f - T_r) \end{aligned} \tag{11}$$

We make (3) and (4) dimensionless using the non-dimensional parameters defined as

$$T^* = \frac{T}{T_i}, \; T_s^* = \frac{T_s}{T_i}, \; T_f^* = \frac{T_f}{T_i}, \; t^* = \frac{u_i t}{L}, \; x^* = \frac{x}{L}, \; p^* = \frac{p}{p_i} \text{ and } u^* = \frac{u}{u_i} \tag{12}$$

where L is the distance between production and injection well. Let, $M_1 = (1-\phi)\rho_s c_{ps}$, $M_2 = \phi\rho_f c_{pf}$ and using equation (12), the dimensionless form of equations (3) and (4) are given as

$$\frac{\partial T_s^*}{\partial t^*} - \frac{k_s}{M_1 L u_i}\frac{\partial^2 T_s^*}{\partial x^{*2}} + \frac{h_c L}{u_i M_1}\left(T_s^* - T_f^*\right) = 0 \tag{13}$$

$$\frac{\partial T_f^*}{\partial t^*} + \frac{u^*}{\phi}\frac{\partial T_f^*}{\partial x^*} - \frac{k_f}{M_2 u_i L}\frac{\partial^2 T_f^*}{\partial x^{*2}} + \frac{h_c L}{M_2 u_i}\left(T_f^* - T_s^*\right) = 0 \tag{14}$$

.

These two partial differential equations should be solved simultaneously to find the temperature distribution for fluid, T_f^* and rock matrix, T_s^* in the formation. These equation are subjected to

$$\begin{aligned} &T_f(x,0) = T_s(x,0) = T_i \quad \text{in dimensionl ess form as} \quad T_f^*(x,0) = T_s^*(x,0) = 1 \\ &T_f(0,t) = T_s(0,t) = T_{steam} \quad // \quad T_f^*(0,t) = T_s^*(0,t) = T_{steam}/T_i \\ &T_f(L,t) = T_s(L,t) = T_i \quad // \quad T_f^*(L,t) = T_s^*(L,t) = 1 \end{aligned} \tag{15}$$

that present the initial and boundary conditions.

If the temperature of the fluid and rock matrix are the same, the energy balance equations can be combined. Combining equation (3) and equation (4) for both fluid and rock matrix in the formation, the energy balance is given in single equation as

$$\left\{\phi\rho_f c_{pf} + (1-\phi)\rho_s c_{ps}\right\}\frac{\partial T}{\partial t} + \rho_f c_{pf} u\frac{\partial T}{\partial x} - \left(k_s + k_f\right)\frac{\partial^2 T}{\partial x^2} = 0 \tag{16}$$

Using equation (10) and the dimensionless parameters in equation (12), equation (16) reduces to

$$\frac{\partial T^*}{\partial t^*} + \frac{\rho_f c_{pf}}{M}\left(u^*\right)\frac{\partial T^*}{\partial x^*} - \frac{\left(k_s + k_f\right)}{MLu_i}\frac{\partial^2 T^*}{\partial x^{*2}} = 0 \quad . \tag{17}$$

This equation gives the dimensionless temperature profile along the formation length when the rock and fluid temperature are same. The initial and boundary conditions are

$$T^*(x,\ 0)=1,\ \ T^*(0,\ t)=T_{steam}/T_i \quad \text{and} \quad T^*(L,\ t)=1. \tag{18}$$

Darcy's law can be written in a dimensionless form according to the definition of dimensionless parameters of equation (12) as $u^* = -(p_i k/u_i L\,\mu)\partial p^*/\partial x^*$. Accordingly, the velocity of the fluid may be written as $u^* = a\ g(t^*)$. Hence, the coefficient *a* is a function of the initial reservoir pressure, distance between injection and production wells, initial injection velocity, permeability of the media, viscosity of the fluid and pressure gradient of the formation. The formation velocity is considered as a linear function of time, $u^* = a\,t^*$.

NUMERICAL SIMULATION

The dimensionless temperature profiles are obtained by solving the equations (13) and (14) simultaneously when we consider that fluid and rock matrix temperatures are different. Equation (17) is solved for the temperature profile when fluid and rock matrix temperatures are the same. These dimensionless temperature profiles with respect to dimensionless space and time are obtained numerically with the finite difference method using implicit scheme. The equation (13) can be written as

$$\frac{\partial T_s^*}{\partial t^*} + a_4 \frac{\partial^2 T_s^*}{\partial x^{*2}} + a_5\left(T_s^* - T_f^*\right) = 0$$

where $a_4 = -\dfrac{k_s}{M_1 L u_i}$ and $a_5 = \dfrac{h_c L}{M_1 u_i}$

Using finite difference method, the equation can be written as;

$$\frac{T_{si}^{*n+1} - T_{si}^{*n}}{\Delta t^*} + a_4 \frac{T_{s(i+1)}^{*n} - 2T_{si}^{*n} + T_{s(i-1)}^{*n}}{\left(\Delta x^*\right)^2} + a_5\left(T_{si}^{*n} - T_{fi}^{*n}\right) = 0$$

$$T_{si}^{*n+1} = T_{si}^{*n} - a_4 \frac{\Delta t^*}{\left(\Delta x^*\right)^2}\left(T_{s(i+1)}^{*n} - 2T_{si}^{*n} + T_{s(i-1)}^{*n}\right) - a_5 \Delta t^*\left(T_{si}^{*n} - T_{fi}^{*n}\right)$$

$$T_{si}^{*n+1} = T_{si}^{*n}\left(1 + 2a_4 \frac{\Delta t^*}{\left(\Delta x^*\right)^2} - a_5 \Delta t^*\right) + T_{s(i+1)}^{*n}\left(-a_4 \frac{\Delta t^*}{\left(\Delta x^*\right)^2}\right) + T_{s(i-1)}^{*n}\left(-a_4 \frac{\Delta t^*}{\left(\Delta x^*\right)^2}\right) + a_5 \Delta t^* T_f^{*n}$$

$$T_{si}^{*n+1} = T_{si}^{*n}\left(1+2a_4h-a_5\Delta t^*\right)+T_{s(i+1)}^{*n}\left(-a_4h\right)+T_{s(i-1)}^{*n}\left(-a_4h\right)+a_5\Delta t^*T_f^{*n}$$

Now let, $a_2 = -a_4h$ and $a_3 = a_5\Delta t^*$. The above equation becomes;

$$T_{si}^{*n+1} = T_{si}^{*n}\left(1-2a_2-a_3\right)+a_2T_{s(i+1)}^{*n}+a_2T_{s(i-1)}^{*n}+a_3T_f^{*n}$$

Again let, $a_1 = 1-2a_2-a_3$ and put the value in the above equation

$$T_{si}^{*n+1} = a_1T_{si}^{*n}+a_2T_{s(i+1)}^{*n}+a_2T_{s(i-1)}^{*n}+a_3T_f^{*n} \tag{19}$$

Equation 19 can be written in terms of programming language which becomes;

$$T_s^*\left(j+1,i\right) = T_s^*\left(j,i\right)*a_1+T_s^*\left(j,i+1\right)*a_2+T_s^*\left(j,i-1\right)*a_2+T_f^*\left(j,i\right)*a_3$$

In equation (14), the velocity of the fluid may be written as $u^* = a\,t^*$ and the equation can be written as

$$\frac{\partial T_f^*}{\partial t^*}+\frac{at^*}{\phi}\frac{\partial T_f^*}{\partial x^*}-\frac{k_f}{M_2u_iL}\frac{\partial^2T_f^*}{\partial x^{*2}}+\frac{h_cL}{M_2u_i}\left(T_f^*-T_s^*\right)=0$$

Let, $b_8 = h_cL/M_2u_i$, $b_5 = -k_f/M_2Lu_i$, $b_7 = a/\phi$

The above equation becomes;

$$\frac{\partial T_f^*}{\partial t^*}+\left(b_7t^*\right)\frac{\partial T_f^*}{\partial x^*}+b_5\frac{\partial^2T_f^*}{\partial x^{*2}}+b_8\left(T_f^*-T_s^*\right)=0$$

Using finite difference method, the equation can be written as;

$$\frac{T_{fi}^{*n+1}-T_{fi}^{*n}}{\Delta t^*}+\left[b_7t^*\right]\frac{T_{f(i+1)}^n-T_{f(i-1)}^n}{2\Delta x^*}+b_5\frac{T_{f(i+1)}^{*n}-2T_{fi}^{*n}+T_{f(i-1)}^{*n}}{\left(\Delta x^*\right)^2}+b_8\left(T_{fi}^{*n}-T_{si}^{*n}\right)=0$$

$$T_{fi}^{*n+1} = T_{fi}^{*n} - \Delta t^{*}\left[b_7 t^{*}\right]\frac{T_{f(i+1)}^{n} - T_{f(i-1)}^{n}}{2\Delta x^{*}} - b_5 \Delta t^{*}\,\frac{T_{f(i+1)}^{*n} - 2T_{fi}^{*n} + T_{f(i-1)}^{*n}}{\left(\Delta x^{*}\right)^2} - b_8 \Delta t^{*}\left(T_{fi}^{*n} - T_{si}^{*n}\right)$$

$$T_{fi}^{*n+1} = T_{fi}^{*n} - \frac{\Delta t^{*}}{\left(\Delta x^{*}\right)^2}\frac{b_7 t^{*}\Delta x^{*}}{2}T_{f(i+1)}^{n} + \frac{\Delta t^{*}}{\left(\Delta x^{*}\right)^2}\frac{b_7 t^{*}\Delta x^{*}}{2}T_{f(i-1)}^{n}$$
$$- b_5\frac{\Delta t^{*}}{\left(\Delta x^{*}\right)^2}\left(T_{f(i+1)}^{*n} - 2T_{fi}^{*n} + T_{f(i-1)}^{*n}\right) - b_8 \Delta t^{*}\left(T_{fi}^{*n} - T_{si}^{*n}\right)$$

Let, $h = \Delta t^{*}/\left(\Delta x^{*}\right)^2$.

$$T_{fi}^{*n+1} = T_{fi}^{*n} - h\frac{b_7 t^{*}\Delta x^{*}}{2}T_{f(i+1)}^{n} + h\frac{b_7 t^{*}\Delta x^{*}}{2}T_{f(i-1)}^{n}$$
$$- b_5 h\left(T_{f(i+1)}^{*n} - 2T_{fi}^{*n} + T_{f(i-1)}^{*n}\right) - b_8 \Delta t^{*}\left(T_{fi}^{*n} - T_{si}^{*n}\right)$$

Now again let, $b_6 = -b_7 \Delta x^{*} t^{*} h/2$, and $b_4 = b_8 \Delta t^{*}$

$$T_{fi}^{*n+1} = T_{fi}^{*n} + b_6 T_{f(i+1)}^{n} - b_6 T_{f(i-1)}^{n} - b_5 h\left(T_{f(i+1)}^{*n} - 2T_{fi}^{*n} + T_{f(i-1)}^{*n}\right) - b_4\left(T_{fi}^{*n} - T_{si}^{*n}\right)$$

$$T_{fi}^{*n+1} = \left(1 + 2b_5 h - b_4\right)T_{fi}^{*n} + \left(b_6 - b_5 h\right)T_{f(i+1)}^{n} - \left(b_6 + b_5 h\right)T_{f(i-1)}^{n} + b_4 T_{si}^{*n}$$

Let, $b_1 = 1 + 2b_5 h - b_4$, $b_2 = b_6 - b_5 h$, and $b_3 = -\left(b_6 + b_5 h\right)$

$$T_{fi}^{*n+1} = b_1 T_{fi}^{*n} + b_2 T_{f(i+1)}^{*n} + b_3 T_{f(i-1)}^{*n} + b_4 T_{si}^{*n} \qquad (20)$$

Equation 20 can be written in terms of programming language which becomes;

$$T_f^*(j+1,i) = T_f^*(j,i)*b_1 + T_f^*(j,i+1)*b_2 + T_f^*(j,i-1)*b_3 + T_s^*(j,i)*b_4$$

In equation (17), the velocity of the fluid may be written as $u^* = a\,t^*$ and the equation can be written as

$$\frac{\partial T^*}{\partial t^*} + \frac{\rho_f c_{pf}}{M}\left(at^*\right)\frac{\partial T^*}{\partial x^*} - \frac{\left(k_s + k_f\right)}{MLu_i}\frac{\partial^2 T^*}{\partial x^{*2}} = 0$$

Let, $c_6 = a\rho_f c_{pf}/M$, $c_7 = -\left(k_S + k_f\right)/MLu_i$ and the above equation becomes;

$$\frac{\partial T^*}{\partial t^*} + c_6 t^* \frac{\partial T^*}{\partial x^*} + c_7 \frac{\partial^2 T^*}{\partial x^{*2}} = 0$$

Using finite difference method, the above equation can be written as;

$$\frac{T_i^{*(n+1)} - T_i^{*n}}{\Delta t^*} + c_6 t^* \frac{T_{i+1}^{*n} - T_{(i-1)}^{n}}{2\Delta x^*} + c_7 \frac{T_{(i+1)}^{*n} - 2T_i^{*n} + T_{(i-1)}^{*n}}{\left(\Delta x^*\right)^2} = 0$$

$$T_i^{*n+1} = T_i^{*n} - \Delta t^* c_6 t^* \frac{T_{(i+1)}^{*n} - T_{(i-1)}^{*n}}{2\Delta x^*} + c_7 \Delta t^* \frac{T_{(i+1)}^{*n} - 2T_i^{*n} + T_{(i-1)}^{*n}}{\left(\Delta x^*\right)^2} = 0$$

$$T_i^{*n+1} = T_i^{*n} - \frac{\Delta t^*}{\left(\Delta x^*\right)^2}\frac{c_6 t^* \Delta x^*}{2} T_{(i+1)}^{*n} + \frac{\Delta t^*}{\left(\Delta x^*\right)^2}\frac{c_6 t^* \Delta x^*}{2} T_{(i-1)}^{*n} - c_7 \frac{\Delta t^*}{\left(\Delta x^*\right)^2}\left(T_{(i+1)}^{*n} - 2T_i^{*n} + T_{(i-1)}^{*n}\right)$$

Let, $c_4 = -c_7 h$, and $c_5 = -c_6 h t^* \Delta x^*/2$

$$T_i^{*n+1} = T_i^{*n} + c_5 T_{(i+1)}^{*n} - c_5 T_{(i-1)}^{*n} + c_4\left(T_{(i+1)}^{*n} - 2T_i^{*n} + T_{(i-1)}^{*n}\right)$$

$$T_i^{*n+1} = \left(1 - 2c_4\right)T_i^{*n} + \left(c_5 + c_4\right)T_{(i+1)}^{*n} + \left(c_4 - c_5\right)T_{(i-1)}^{*n}$$

Let, $c_1 = 1 - 2c_4$, $c_2 = c_5 + c_4$, $c_3 = c_4 - c_5$,

Therefore,

$$T_i^{*n+1} = c_1 T_i^{*n} + c_2 T_{i+1}^{*n} + c_3 T_{i-1}^{*n} \tag{21}$$

This equation can be written as

$$T(j+1,i) = T(j,i) * c_1 + T(j,i+1) * c_2 + T(j,i-1) * c_3$$

RESULTS AND DISCUSSION

The computations are carried out for a reservoir of $L = 500$ ft. The steam is injected through a $7''$ well diameter. The properties of the rock and fluids are given in Table 1. It is taken into account that $\Delta x^* = 0.02$, $\Delta t^* = 0.0001$.

The variations of temperatures are obtained for two cases. At first, it is assumed that the fluid and rock temperature are same. In the second case, the variations of the fluid and rock temperatures are obtained separately. The computations are carried out for different fluid velocities. It is taken into account that the velocity coefficient is $a = 0.04108,$ 0.035, 0.03, 0.025, 0.02, 0.01, 0.001 and 0.0001. The effects of the injected steam velocity are also investigated by changing the rate of the steam. It is taken into account that $u_i = 0.1217\ ft/\sec$ *0.085* $ft/\sec$, *0.049* $ft/\sec$, *0.024* $ft/\sec$, *0.012* $ft/\sec$.

Table 1 Fluid and Rock properties value for numerical computation

Fluid and Rock properties	Fluid and Rock properties
c_{pg} = 7.1 [$Btu/lb_m - {}^0F$]	S_g = 20% [vol/vol]
c_{po} = 0.5 [$Btu/lb_m - {}^0F$]	S_o = 60% [vol/vol]
c_{ps} = 0.21 [$Btu/lb_m - {}^0F$]	S_w = 20% [vol/vol]
c_{pw} = 1.0 [$Btu/lb_m - {}^0F$]	$T_{steam} = 500\left[{}^0F\right]$
h_c = 13.74 [$Btu/hr - ft^2 - {}^0F$]	$T_i = 150\ \left[{}^0F\right]$
k_g = 0.0023 [$Btu/hr - ft - {}^0F$]	$\rho_g = 1.0433[\mathrm{lb_m}/\mathrm{ft}^3]$
K_i = 100.0 [*md*]	ρ_o = 50.0 [lb_m/ft^3]
k_0 = 0.22408 [$Btu/hr - ft - {}^0F$]	ρ_s =167.0 [lb_m/ft^3]
k_s = 1.5 [$Btu/hr - ft - {}^0F$]	ρ_w = 62.5 [lb_m/ft^3]
k_w = 0.606 [$Btu/hr - ft - {}^0F$]	ϕ = 25% [*vol/vol*]
$p_i = 4000\ [\mathrm{psia}\ ]$	$\mu_f = 10000\,[\mathrm{cp}]$

Temperature variation with distance and time for fluid velocity

The variation of dimensionless temperature along the length of the reservoir is depicted in Figs. 2a & 2b for a = 0.04108 and 0.0001, respectively, when $u_i = 0.1217\ ft/\text{sec}$ for different time steps and $T_s = T_f$. At the beginning of the steam injection, the reservoir formation heats up only around the injection wellbore. For low velocity, reservoir temperature goes up gradually with time. However, if the fluid velocity goes up, the overall reservoir temperature goes up faster with time. Temperature distribution along x-direction can be separated into three zones, steam zone, hot water zone, and unaffected zone. For low velocity, the steam zone is steeper, the hot water zone is only a little wider and the unaffected zone is almost 50% of the reservoir, whereas for high velocity, steam zone and hot water zone become gradually widen with time.

The temperature profile is depicted in Figs. 3a & 3b when $T_s \neq T_f$. The same trend is shown in this situation. The difference between rock and fluid temperature is very small in the range of 10^{-3}. The profile of temperature shows that the reservoir temperature is going up in this case.

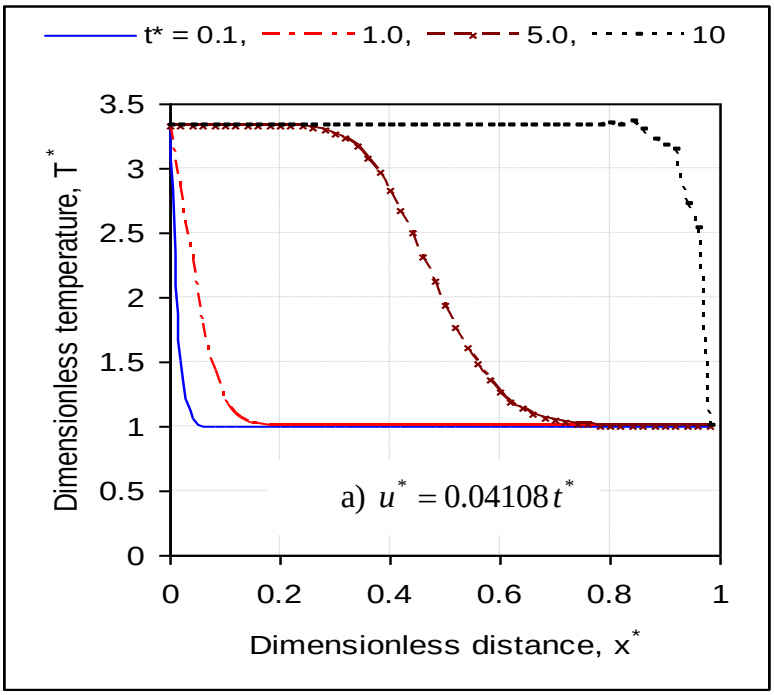

Figure 2 Temperature variation as a function of distance for case I

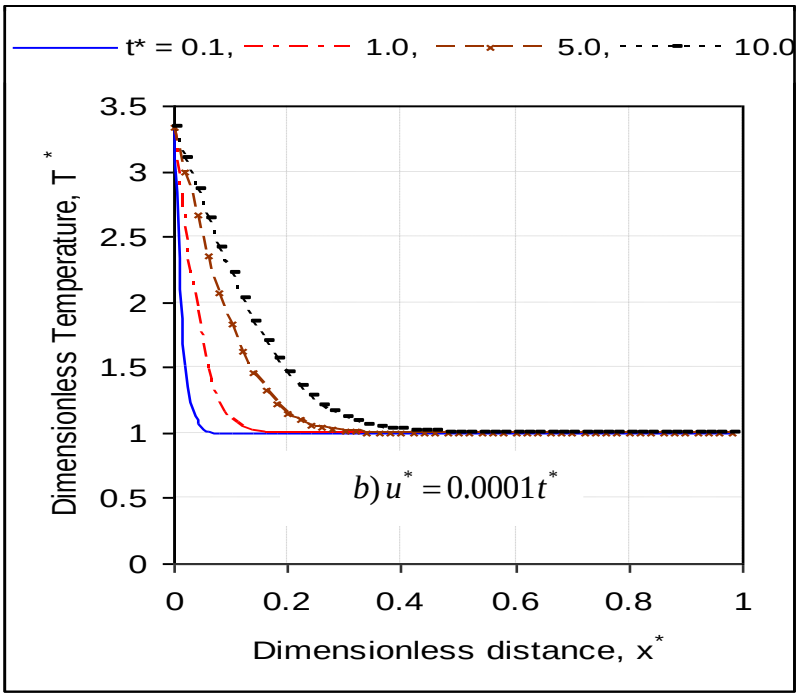

Figure 2 Temperature variation as a function of distance for case I

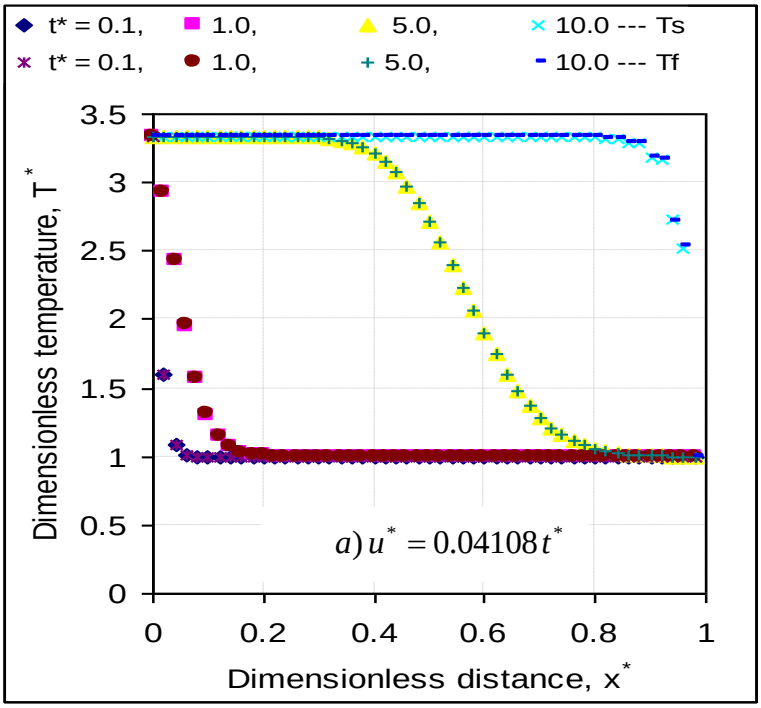

Figure 3 Temperature variations as a function of distance for case II

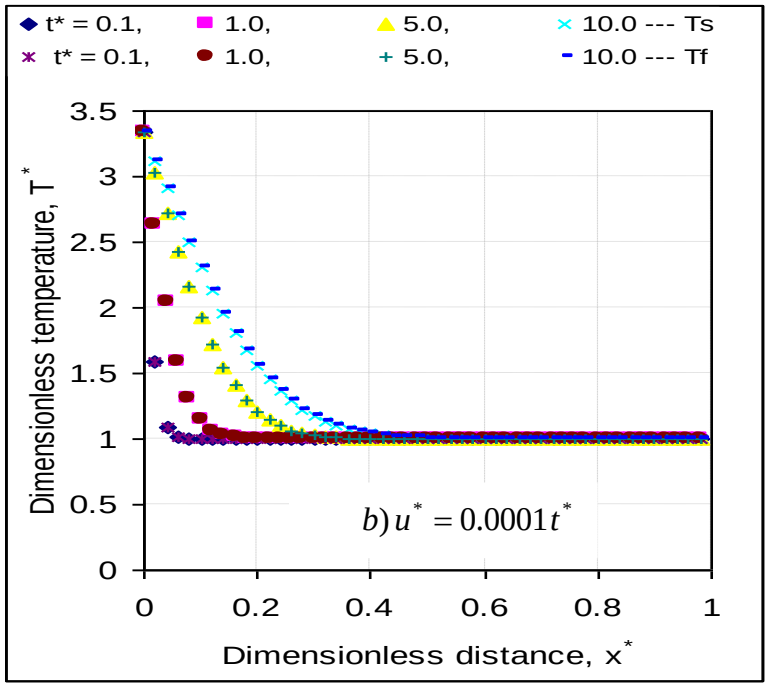

Figure 3 Temperature variations as a function of distance for case II

The variation of dimensionless temperature with time of the reservoir is shown in Figs. 4a & 4b for a = 0.04108 and 0.0001 and $u_i = 0.1217\ ft/\text{sec}$ at different distances when $T_s = T_f$. When fluid velocity is low, reservoir temperature does not propagate evenly for long time after its 50% distance. However, temperature increases gradually around the wellbore. If the fluid velocity is increased, the propagation is higher and temperature goes up rapidly with time and reaches its maximum temperature after a longer time.

The temperature profile is depicted in Figs. 5a & 5b when $T_s \neq T_f$. Almost the same trend is shown in this situation. The difference between rock and fluid temperature is very small in the range of 10^{-3}. The profile of temperature shows that the reservoir temperature is going up and rises faster with time for both situations in comparison with the first case.

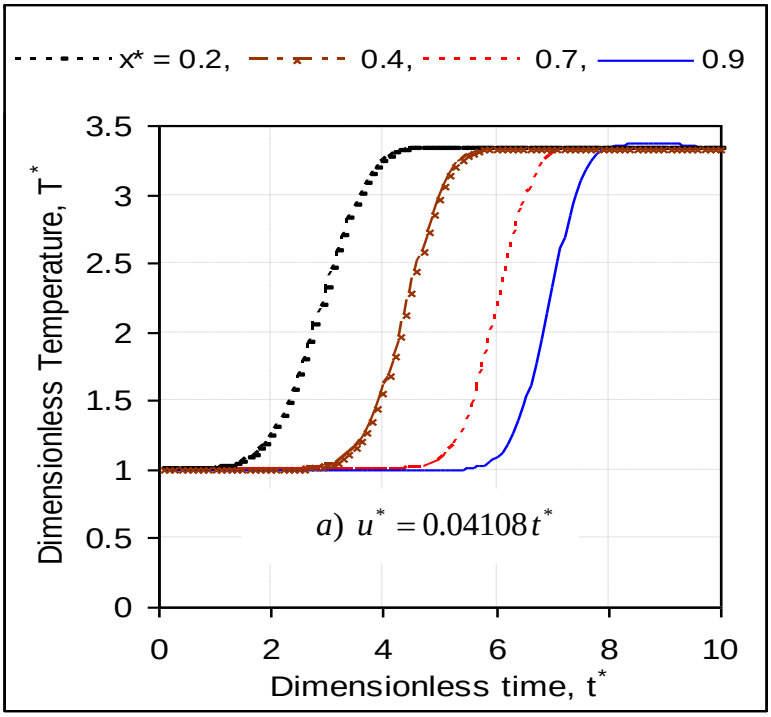

Figure 4 Temperature variations as a function of time for case I

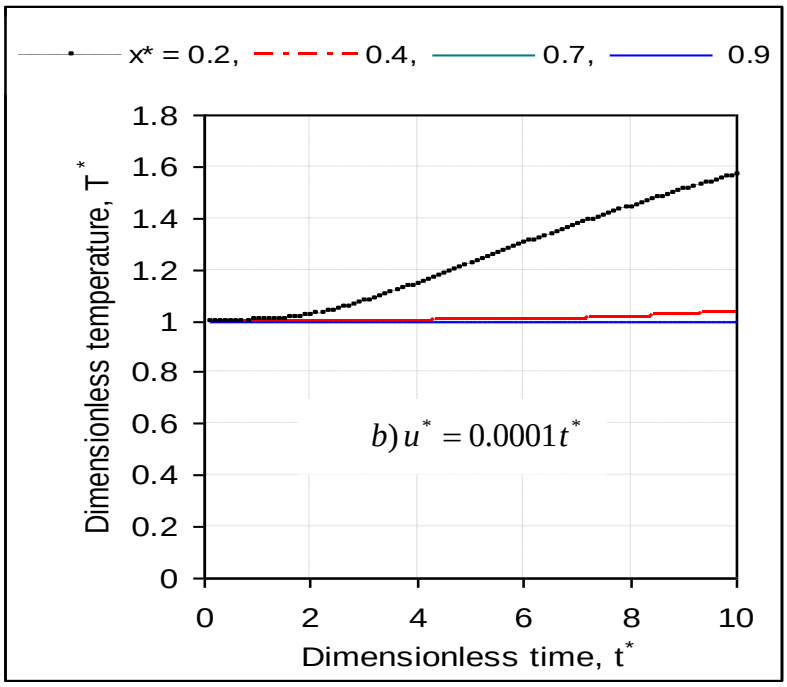

Figure 4 Temperature variations as a function of time for case I

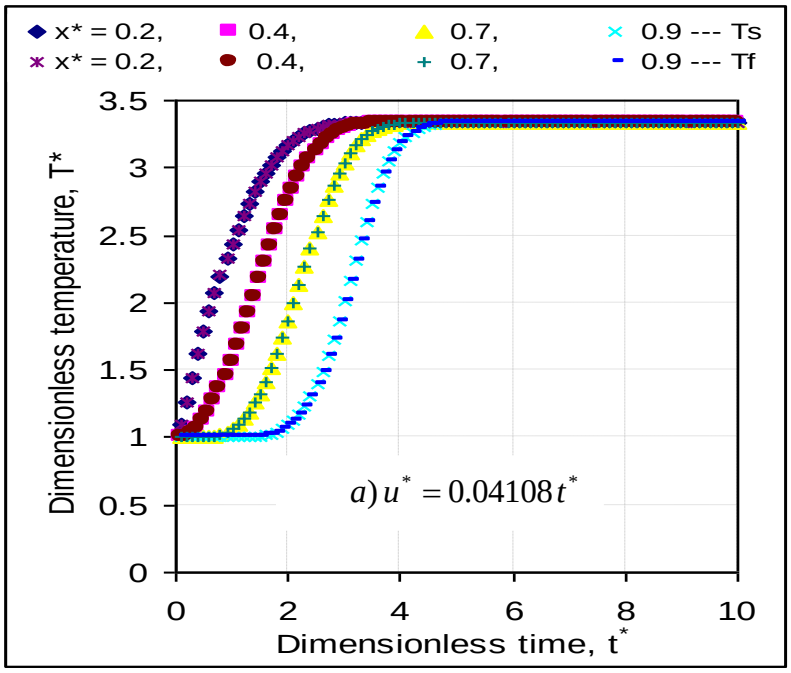

Figure 5 Temperature variations as a function of time for case II

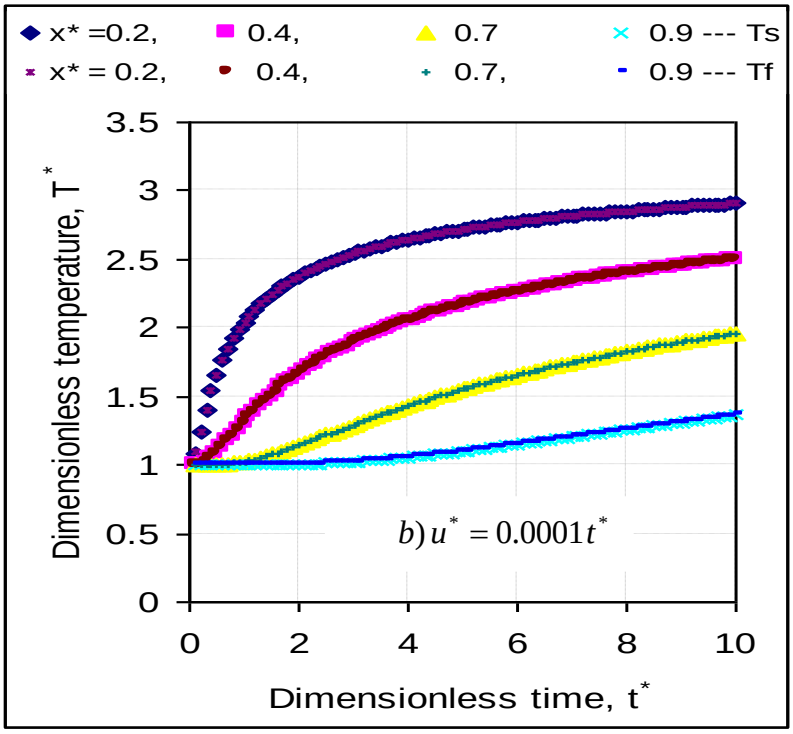

Figure 5 Temperature variations as a function of time for case II

Effects of fluid velocity on temperature with time and along distance

The variation of dimensionless temperature along the length of the reservoir is presented in Figs. 6a & 6b for different fluid velocity. This is for the same fluid and rock temperature. Here, $u_i = 0.1217\ ft/\sec$ is taken into account. At the beginning of the steam injection, formation velocity has less impact on temperature distribution and it does not heat up very far away from the injection well. However, as time goes up the reservoir formation heats up gradually and goes deeper into the formation. If formation velocity goes down, the temperature profile cannot propagate further with respect to space.

Figs. 7a & 7b represent in the same way for the same conditions when $T_s \neq T_f$. The pattern of the graph is almost the same as the first case. This indicates that if fluid and rock temperatures are different, this criterion has less impact on the temperature propagation. However, this consideration makes the propagation somewhat faster and more in line with the first case. This indicates that the fluid convection effects are less important than conduction.

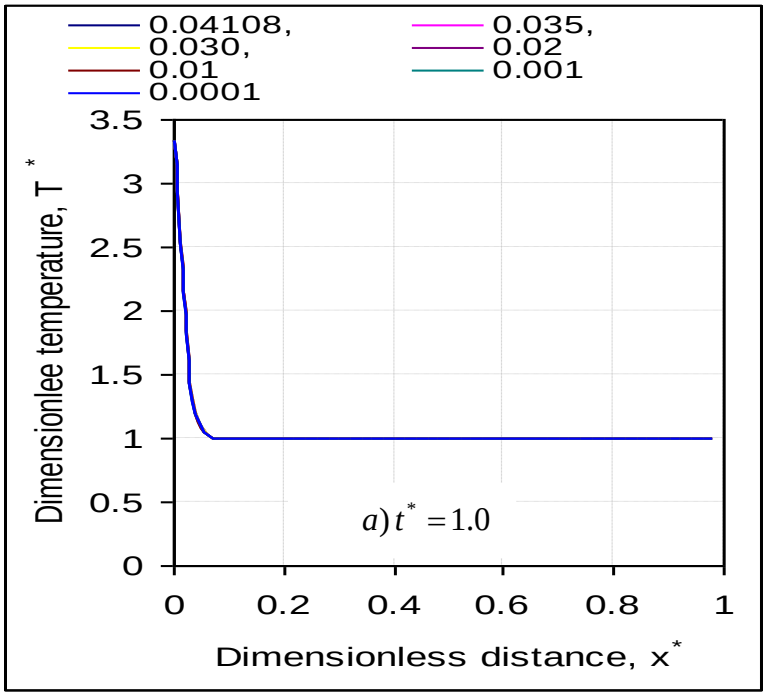

Figure 6 Temperature variations for different fluid velocity as a function of distance for case I

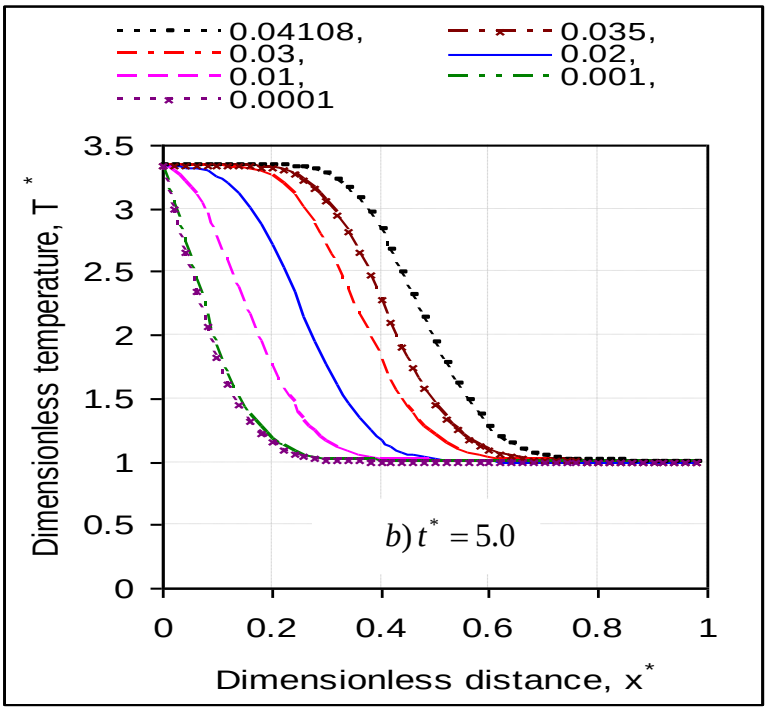

Figure 6 Temperature variations for different fluid velocity as a function of distance for case I

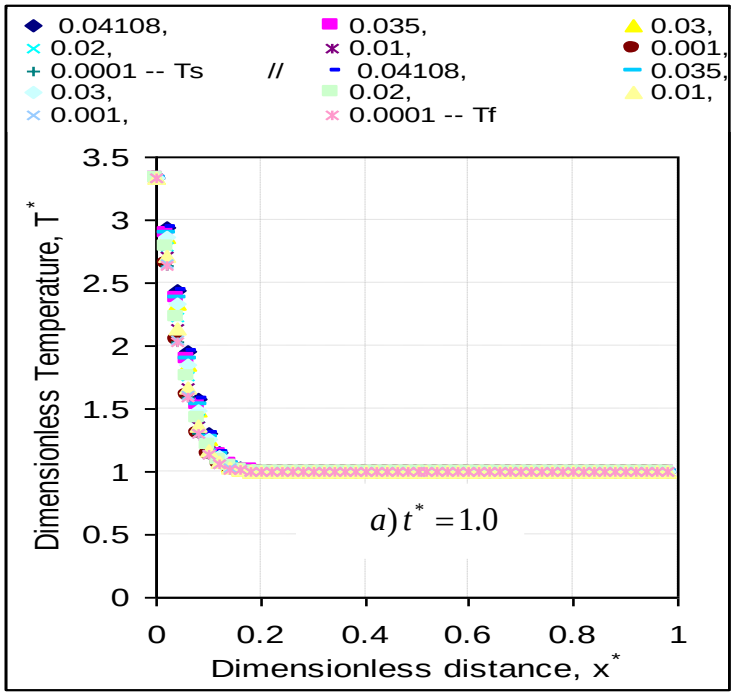

Figure 7 Temperature variations for different fluid velocity as a function of distance for case II

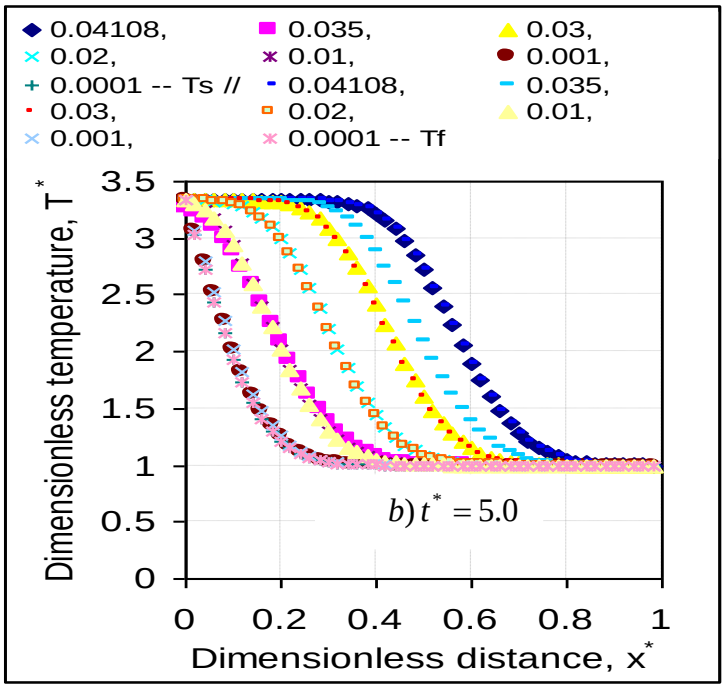

Figure 7 Temperature variations for different fluid velocity as a function of distance for case II

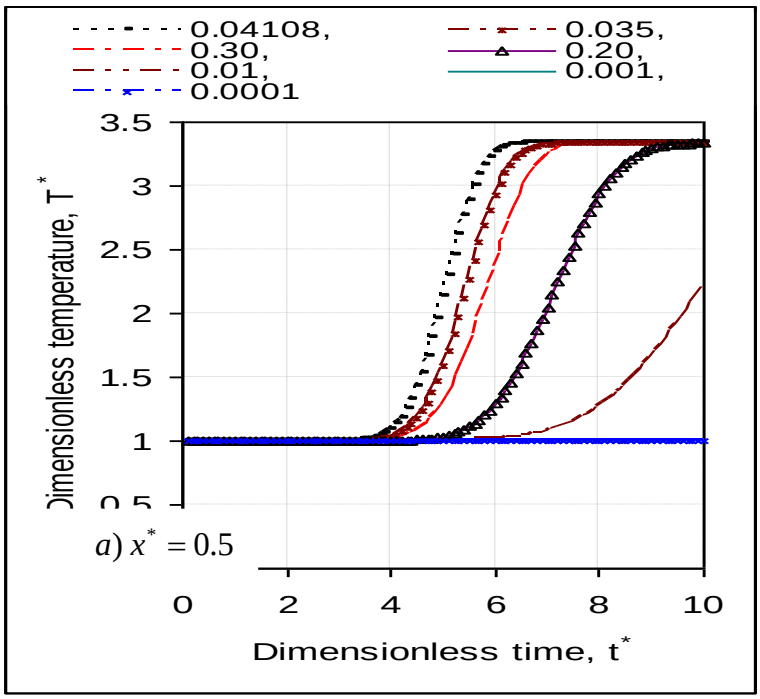

Figure 8 Temperature variations for different fluid velocity as a function of time for case I

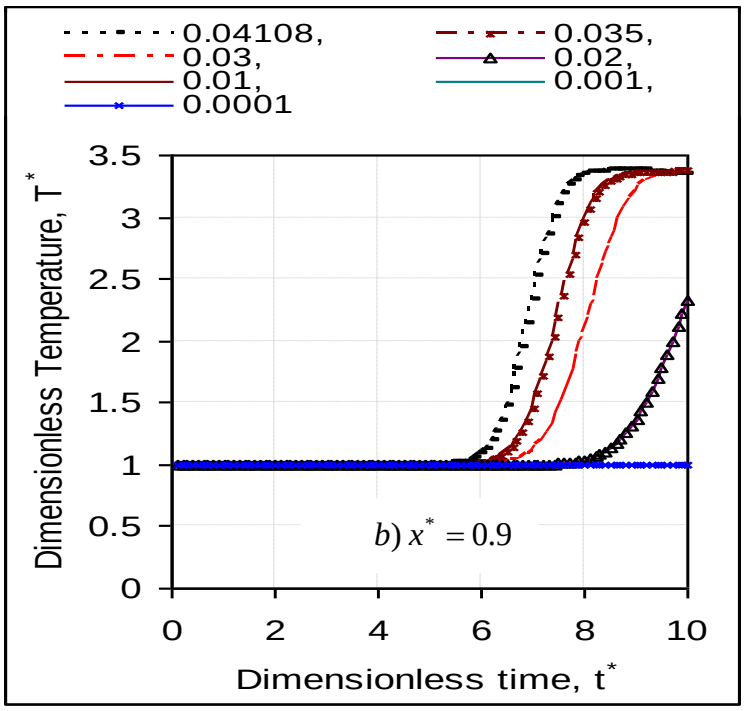

Figure 8 Temperature variations for different fluid velocity as a function of time for case I

The variation of dimensionless temperature with dimensionless time of the reservoir is presented in Figs. 8a & 8b for different fluid velocity. This is for the same fluid and rock temperature. Here, $u_i = 0.1217\ ft/\text{sec}$ is taken into account. It is very clear that fluid velocity has a strong influence on temperature propagation. The reservoir heats up quickly with time and reaches its injected steam temperature depending on the time and velocity of fluid. When velocity of fluid decreases, the reservoir does not heat up faster and remains almost the same as the initial reservoir temperature for low fluid velocity. At the beginning of the steam injection, formation velocity has less impact on temperature distribution and it does not heat up very far away from the injection well. However, as time passes the reservoir formation heats up gradually and goes deeper to the formation. If formation velocity goes down, the temperature profile cannot propagate further with respect to space.

Figs. 9a & 9b represents same for the same conditions when $T_s \neq T_f$. Fluid velocity has more effect on the temperature profile in this case compared with the other case. The reservoir heats up faster in less time than case two. Temperature profile propagates gradually with time even at low fluid velocity. The difference between rock and fluid temperatures is not very significant throughout these fluid velocity changes.

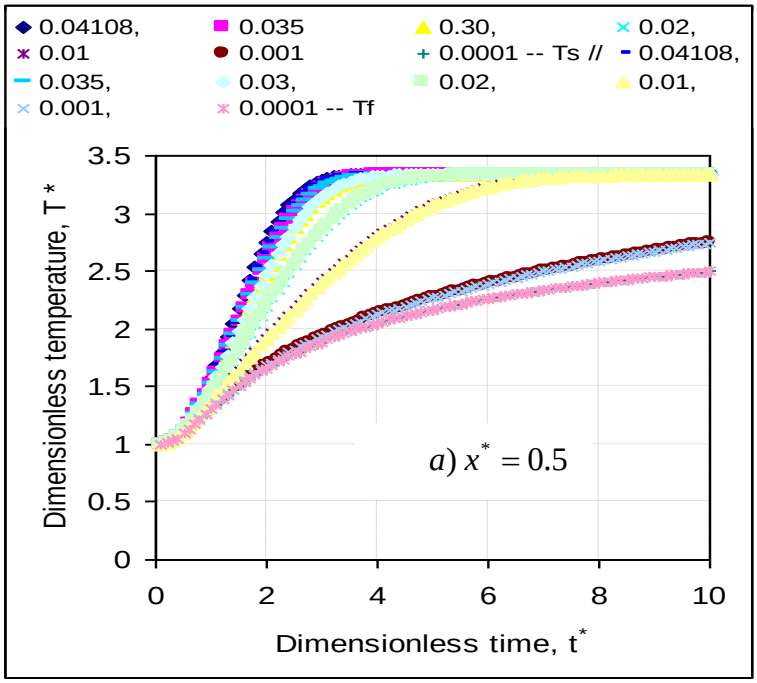

Figure 9 Temperature variations for different fluid velocity as a function of time for case II

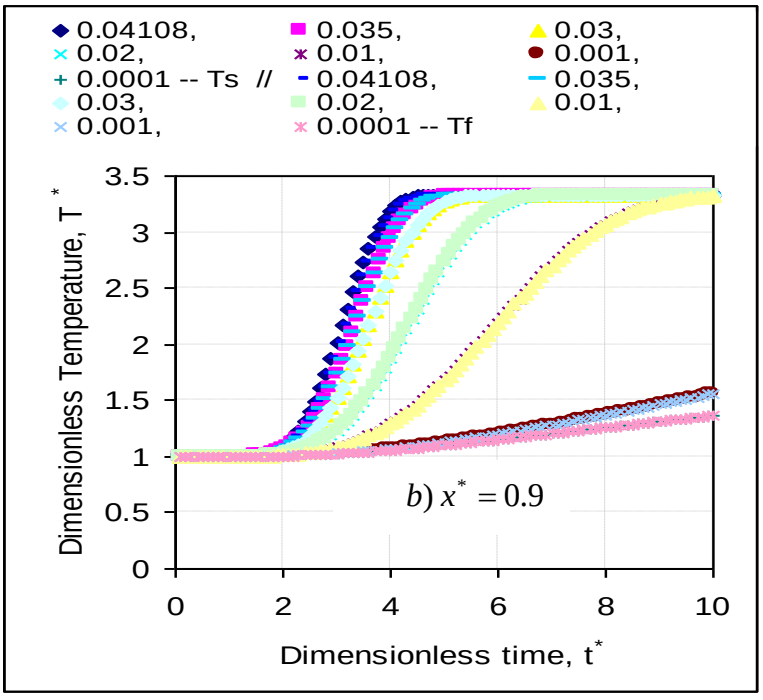

Figure 9 Temperature variations for different fluid velocity as a function of time for case II

Temperature variation with distance and time for initial steam velocity

The variation of dimensionless temperature along the length of the reservoir is depicted in Figs. 10a & 10b for $u_i = 0.1217\ ft/\sec$ and $u_i = 0.01217\ ft/\sec$ respectively when for $u^* = 0.01\ t^*$ at different time steps when $T_s = T_f$. At the beginning of the steam injection, the reservoir formation heats up only around the injection wellbore. For low velocity, reservoir temperature goes up gradually with time. If the injection steam velocity decline, the overall reservoir temperature goes up faster with time.

The temperature profile is shown Figs. 11a & 11b when $T_s \neq T_f$. These plotting are for $u_i = 0.1217\ ft/\sec$ and $u_i = 0.024\ ft/\sec$ because numerical computation does not work properly when initial steam velocity is beyond this level. Initial steam velocity has more influence on temperature profile when fluid and rock temperatures are different. However, there is no significant change between these two temperatures. Temperature distribution propagates more than case I for any time step. Initial steam velocity has more impact on this distribution. When the velocity is low, reservoir heats up quickly at any distance from the reservoir.

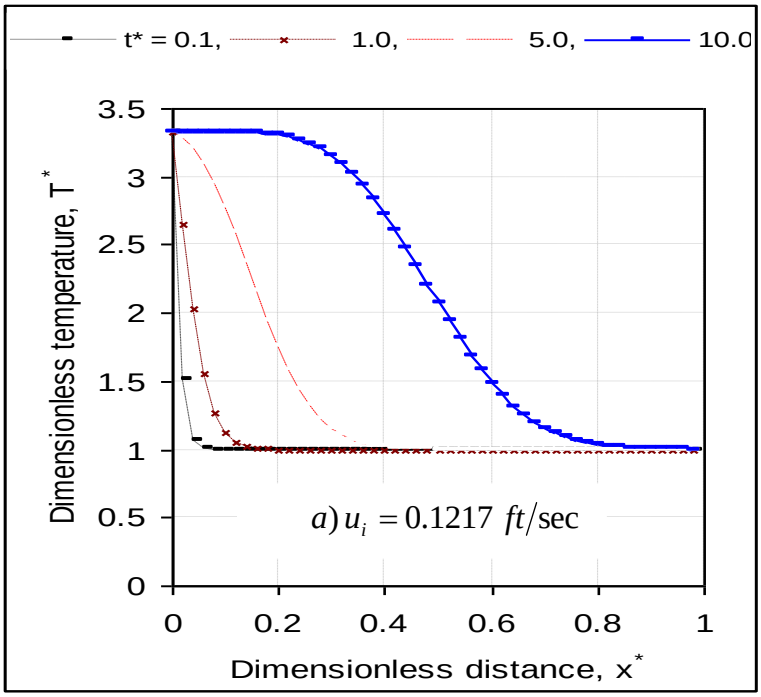

Figure 10 Temperature variations for different steam velocity as a function of distance for case I

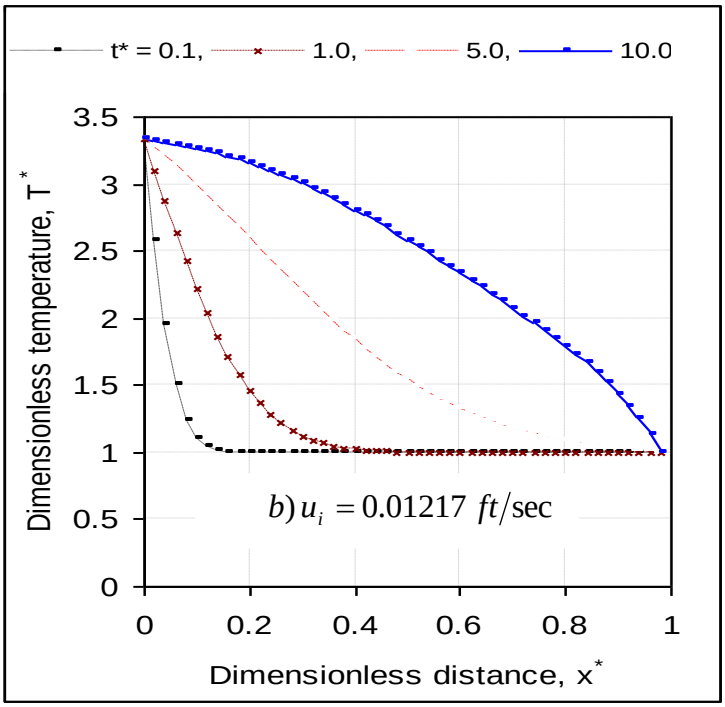

Figure 10 Temperature variations for different steam velocity as a function of distance for case I

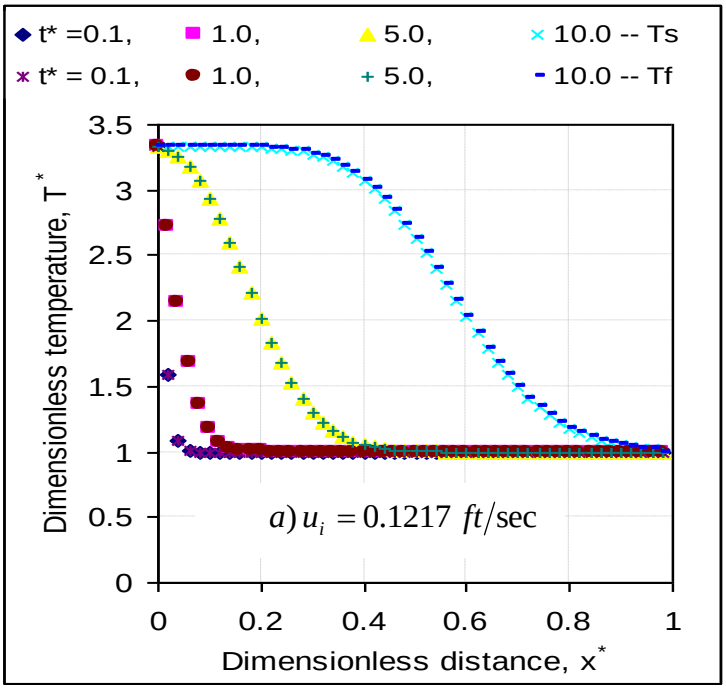

Figure 11 Temperature variations for different steam velocity as a function of distance for case II

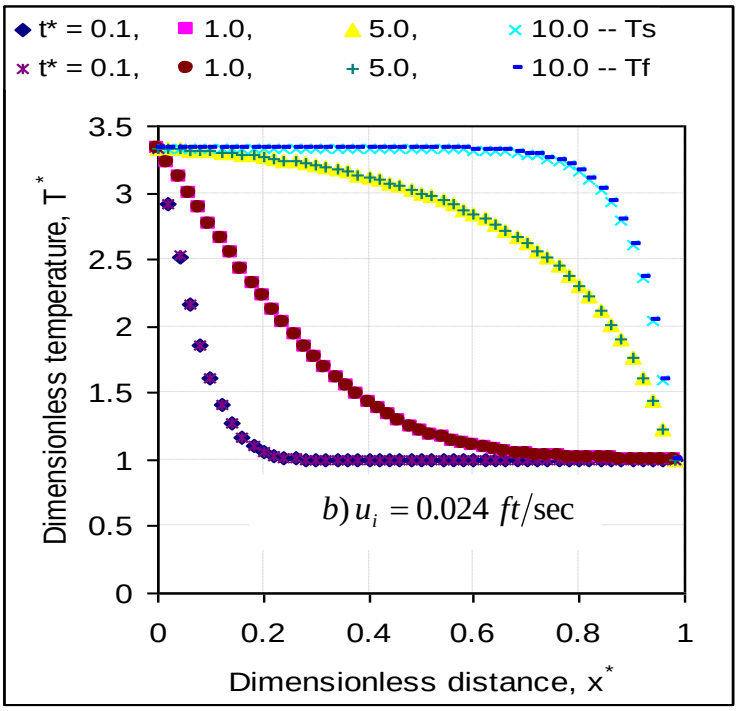

Figure 11 Temperature variations for different steam velocity as a function of distance for case II

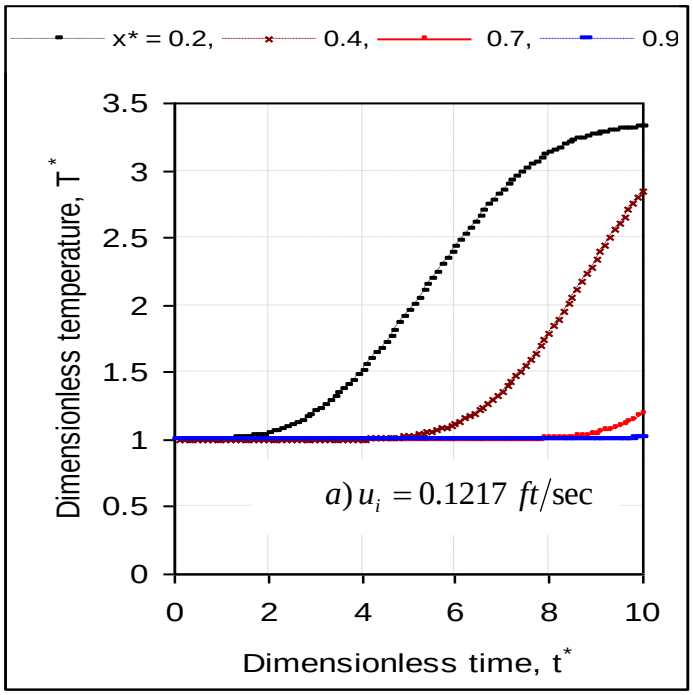

Figure 12 Temperature variations for different steam velocity as a function of time where for case I

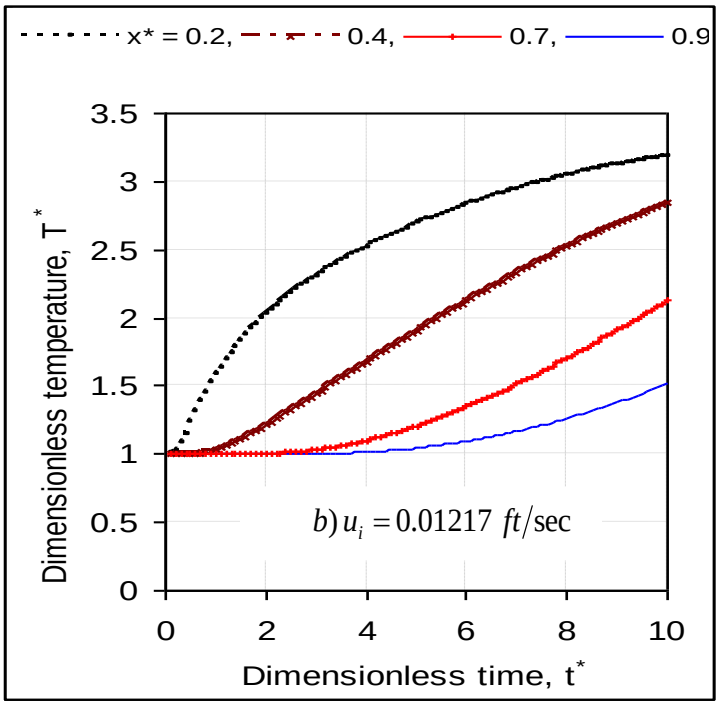

Figure 12 Temperature variations for different steam velocity as a function of time where for case I

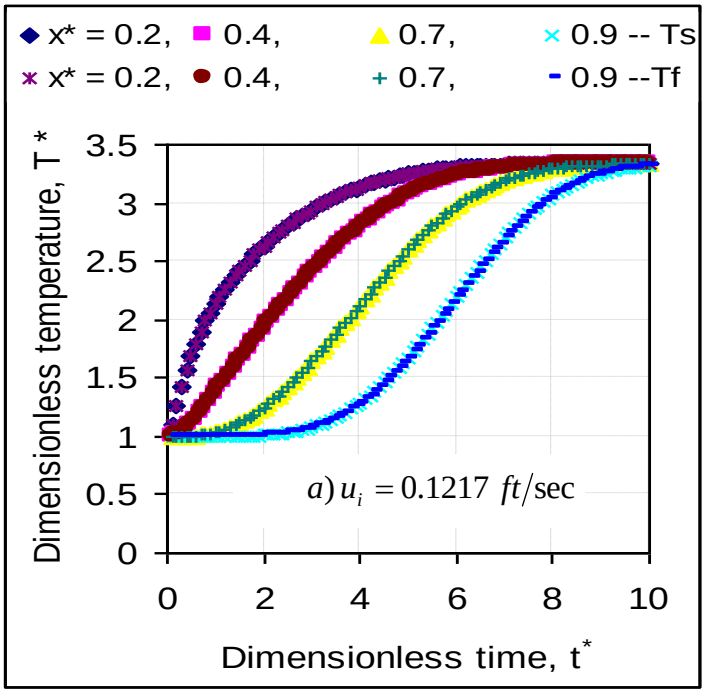

Figure 13 Temperature variations for different steam velocity as a function of time where for case II

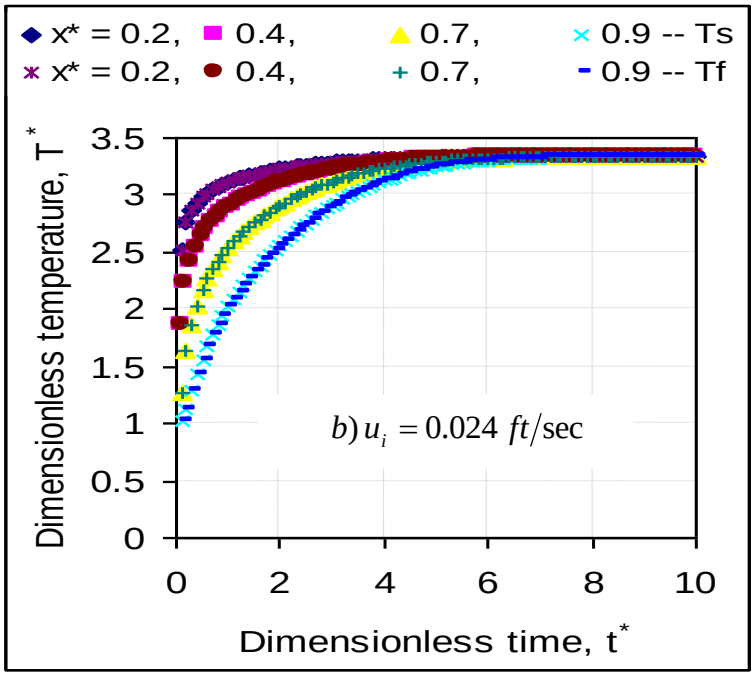

Figure 13 Temperature variations for different steam velocity as a function of time where for case II

The variation of dimensionless temperature with time of the reservoir is shown in Figs. 12a &12b for $u_i = 0.1217\ ft/\sec$ and $u_i = 0.01217\ ft/\sec$ respectively and for $u^* = 0.01\ t^*$ at different distances when $T_s = T_f$. When fluid velocity is low, reservoir temperature goes up gradually with time throughout the reservoir and the pattern is smooth. However, if the velocity is higher, the temperature increases slower than that of low velocity and around the production zone, it does not heat up well.

The temperature profile is depicted in Figs. 13a & 13b when $T_s \neq T_f$. These plotting are for $u_i = 0.1217\ ft/\sec$ and $u_i = 0.024\ ft/\sec$ because numerical computation does not work properly when initial steam velocity is beyond this level. If fluid and rock temperatures are not the same, initial steam velocity has more impact on temperature propagation. Reservoir heats up faster in comparison with case I. In this case, temperature propagation is deeper than case I. If initial velocity is decreased, it takes less time to heat up the whole reservoir and reaches the range of steam velocity in less time.

Effects of initial steam velocity on temperature with time and along distance

The variation of dimensionless temperature along the length of the reservoir is presented in Figs. 14a & 14b for different initial injection velocity. This is for the same fluid and rock temperature. Here, $u = 0.01\ t^*$ is taken into account. At the beginning of the steam

injection, initial steam velocity has less impact on temperature distribution and it does not heat up very far away from the injection well. However, as time progresses the reservoir formation heats up gradually and goes deeper to the formation especially when initial steam velocity is less.

Figs.15a & 15b represent the same for the same conditions when $T_s \neq T_f$. These figures indicate that if fluid and rock temperatures are different, initial steam velocity has less impact on the temperature propagation. The range of temperature difference is within 10^{-3}. At the beginning of steam injection, reservoir heats up gradually. If initial steam velocity becomes less, temperature propagation goes further towards the production well. However, as times increases, the reservoir heats up faster, and for low velocity the trend of the curve is opposite to higher velocity. This behavior of temperature propagation indicates that heat conduction is more active in the reservoir when velocity is less and thus temperature propagation travels more pathways within the reservoir.

The variation of dimensionless temperature with time is presented in Fig. 16a & 16b for different initial injection velocity. These figures are plotted when $T_s = T_f$. Here, $u = 0.01t^*$ is taken into account. As time increases, the reservoir starts to heat up. When velocity decline, reservoir temperature goes up faster for a particular distance. As the distance increases with respect to the injection well, the temperature propagation becomes weaker.

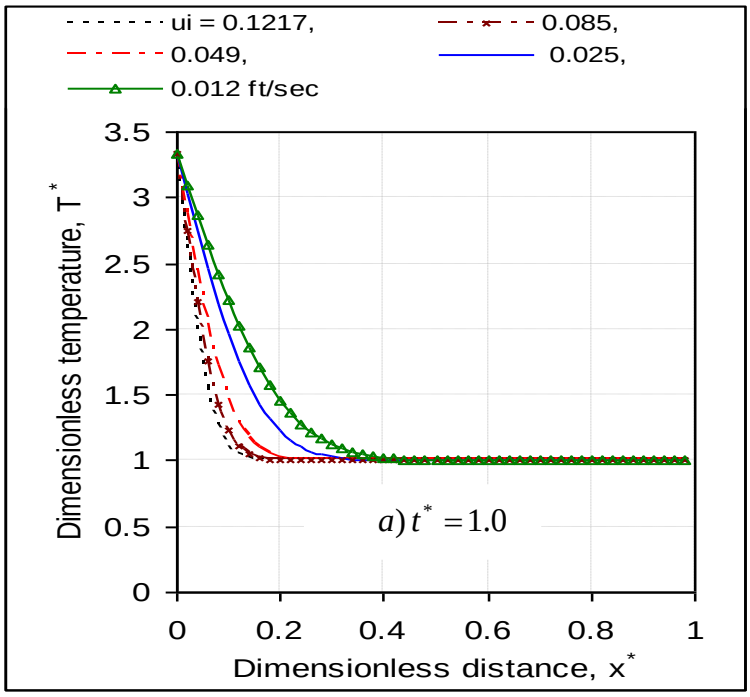

Figure 14 Temperature variations with distance for different steam velocity for case I

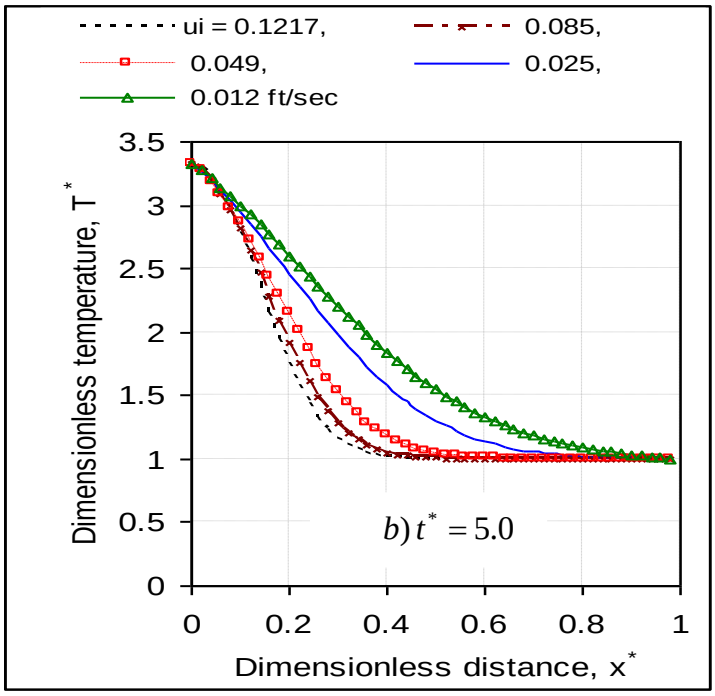

Figure 14 Temperature variations with distance for different steam velocity for case I

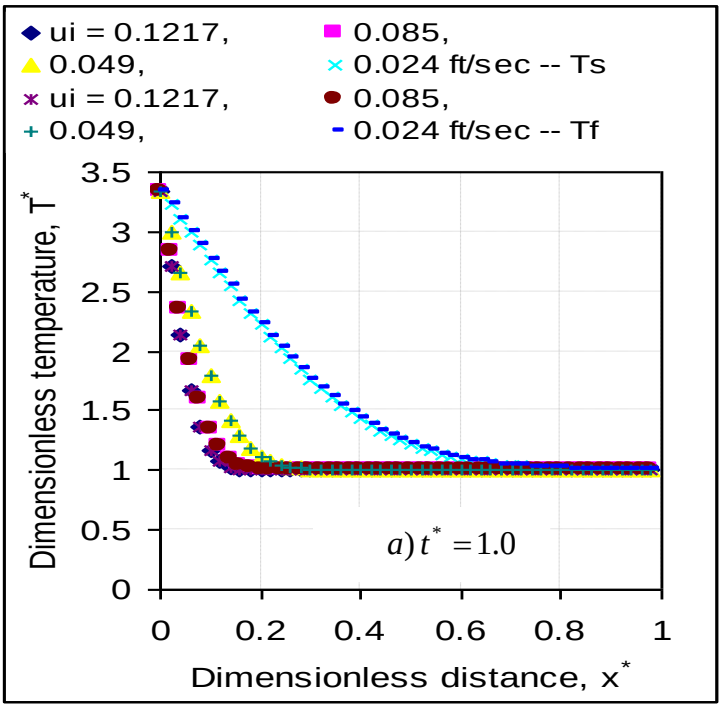

Figure 15 Temperature variations with distance for different steam velocity for case II

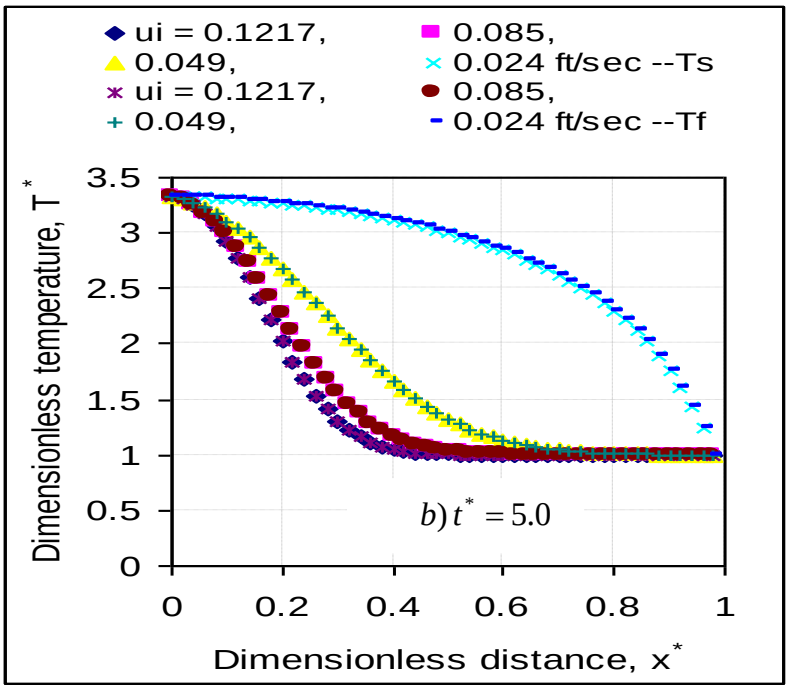

Figure 15 Temperature variations with distance for different steam velocity for case II

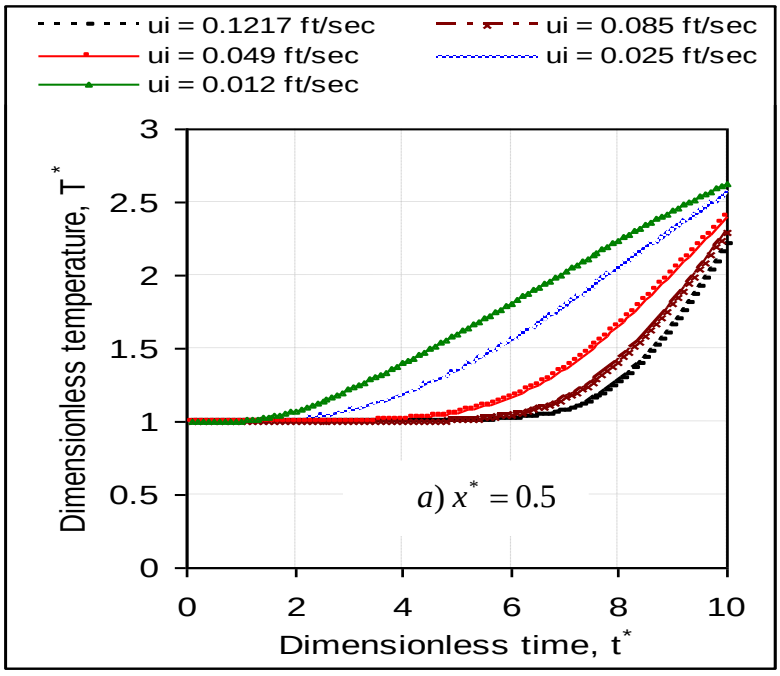

Figure 16 Temperature variations with time for different steam velocity for case I

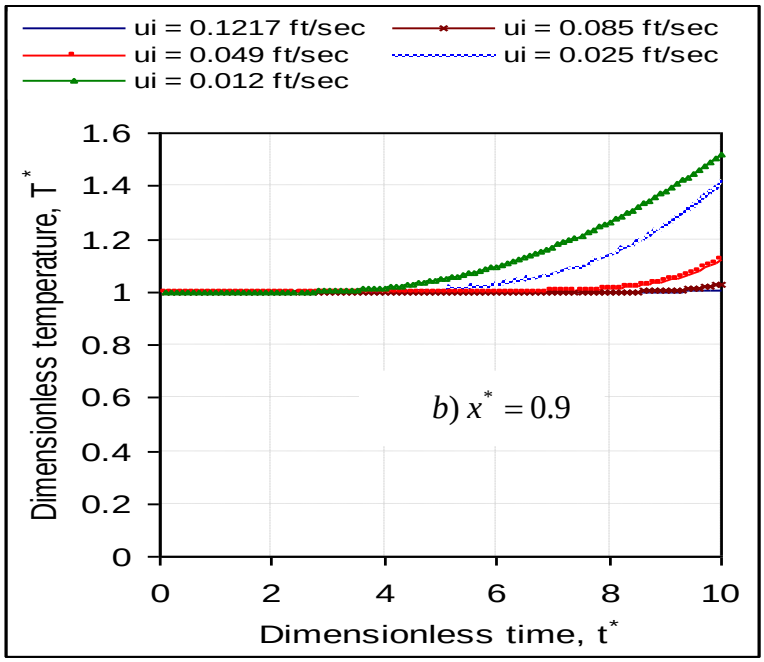

Figure 16 Temperature variations with time for different steam velocity for case I

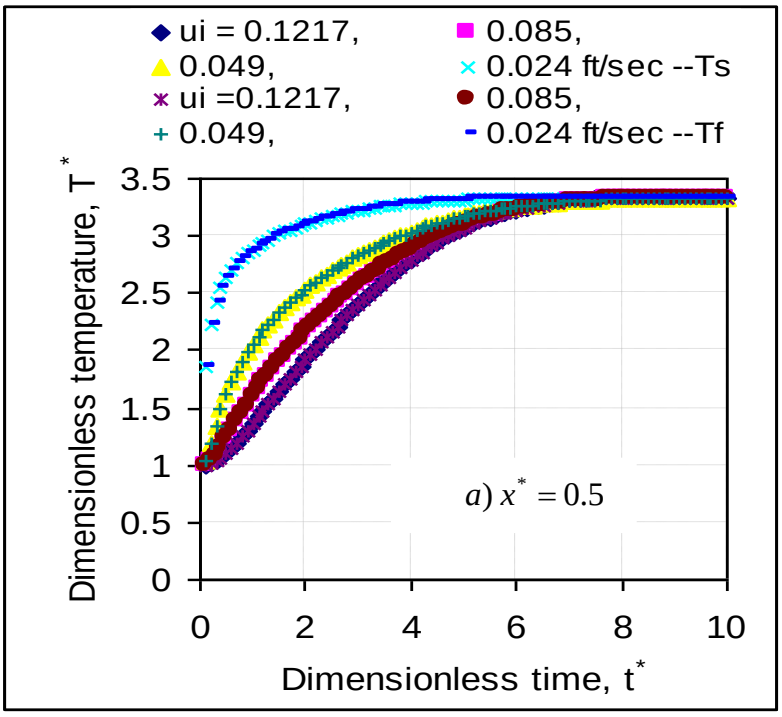

Figure 17 Temperature variations with time for different steam velocity for case II

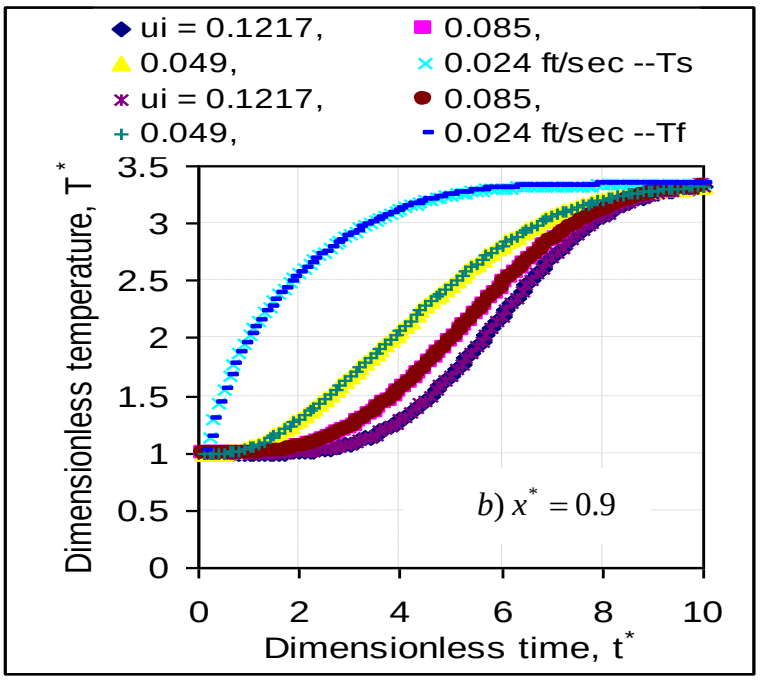

Figure 17 Temperature variations with time for different steam velocity for case II

Figs. 17a & 17b show the same distribution when $T_s \neq T_f$. In this case the pattern and shape of the cure is opposite to case I. Reservoir temperature goes up faster around the injection wellbore. When steam temperature declines, reservoir temperature goes up quickly and reaches steam temperature in a longer time.

CONCLUSION

Energy balance equation for temperature distribution in porous media has been solved using a convection and conduction heat transfer concept when fluid and rock temperatures are considered different and the same. A simultaneous iteration process is used when fluid and rock temperatures are considered to be different. It is found that the fluid and rock matrix temperature difference is negligible. The convection does not play a deciding role in the temperature profile due to very slow motion of fluid inside the medium. It is also sensitive to steam or hot water injection rate or velocity. The temperature distributions along x-direction for various times have also been investigated. The shape and type of the temperature profile is dependent on formation fluid and hot water or steam injection velocity.

ACKNOWLEDGEMENTS

The authors would like to thank the Atlantic Canada Opportunities Agency (ACOA) for funding this project under the Atlantic Innovation Fund (AIF). The first author would also like to thank Natural Sciences and Engineering Research Council of Canada (NSERC) for funding.

NOMENCLATURE

c_{pf} = Specific heat capacity of injected fluid, $Btu/lb_m - {}^0F$

c_{po} = Specific heat capacity of oil, $Btu/lb_m - {}^0F$

c_{ps} = Specific heat capacity of solid rock matrix, $Btu/lb_m - {}^0F$

c_{pw} = Specific heat capacity of water, $Btu/lb_m - {}^0F$

c_{pg} = Specific heat capacity of steam, $Btu/lb_m - {}^0F$

g = gravitational acceleration in *x* direction, $ft/\sec^2$

h_c = convection heat transfer coefficient, $Btu/hr - ft^2 - {}^0F$

H_{oTf} = enthalpy of oil at temperature, T_f, Btu/lb_m

H_{oTi} = enthalpy of oil at temperature, T_i, Btu/lb_m

H_{sTf} = enthalpy of rock at temperature, T_f, Btu/lb_m

H_{sTi} = enthalpy of rock at temperature, T_i, Btu/lb_m

H_{wTf} = enthalpy of water at temperature, T_f, Btu/lb_m

H_{wTr} = enthalpy of water at temperature, T_r, Btu/lb_m

H_{gTf} = enthalpy of steam at temperature, T_f, Btu/lb_m

H_{gTr} = enthalpy of steam at temperature, T_r, Btu/lb_m

K_i = Permeability, *md*

k_f = thermal conductivity of fluid, $Btu/hr - ft - {}^0F$

k_o = thermal conductivity of oil, $Btu/hr - ft - {}^0F$

k_s = thermal conductivity of solid rock matrix, $Btu/hr - ft - {}^0F$

k_w = thermal conductivity of water, $Btu/hr - ft - {}^0F$

k_g = thermal conductivity of steam, $Btu/hr - ft - {}^0F$

L = distance between production and injection well along x direction, ft

L^* = dimensionless length of the reservoir

M = Average volumetric heat capacity of the fluid-saturated rock, $Btu/ft^3 - {}^0F$

Q_g = constant rate of heat generation per unit volume, Btu/ft^3

$q_{inj} = Au$ = injection volume flow rate of steam, *sbl/day*

$q_{prod} = Au$ = production volume flow rate of oil, *sbl/day*

S_{wi} = initial water saturation

S_w = water saturation, volume fraction

S_g = Gas saturation, volume fraction

S_o = oil saturation, volume fraction

t = time, *hr*

T = Temperature, ${}^oF$

T_f = Temperature of injected fluid, ${}^oF$

T_i = initial reservoir temperature, ${}^oF$

T_r = Reference temperature of injected fluid, ${}^oF$

T_s = Average temperature of solid rock matrix, ${}^oF$

t^* = dimensionless time

T^* = dimensionless temperature

u = filtration velocity in x direction, $ft/\sec$

u^* = dimensionless velocity

x^* = dimensionless distance

ϕ = Porosity of the rock, volume fraction

ρ = reference density, lb_m/ft^3

ρ_f = density of fluid, lb_m/ft^3

ρ_o = density of oil, lb_m/ft^3

ρ_s = density of solid rock matrix, lb_m/ft^3

ρ_w = density of water, lb_m/ft^3

ρ_g = density of steam, lb_m/ft^3

REFERENCES

Akin, S. 2004. Mathematical Modeling of Steam Assisted Gravity Drainage. SPE - 86963, presented at SPE International Thermal Operations and Heavy Oil Symposium and Western Regional Meeting, held in Bakersfield, California, USA, March 16 – 18.

Akkutlu, I. Y. and Yortsos, Y.C. 2005. The Effect of Heterogeneity on In-Situ Combustion: Propagation of Combustion Fronts in Layered Porous media. SPE Journal, December, 394 – 404.

Atkinson, P.G. and Ramey Jr., H.J. 1977. Problems of Heat Transfer in Porous Media. SPE – 6792, presented at the 52nd Annual Fall Technical Conference and Exhibition of the Society of Petroleum Engineers of AIME, held in Denver, Colorado, October 9 -12.

Canbolat, S. Akin, S. and Kovscek A.R. 2004. Noncondensable gas steam-assisted gravity drainage", *Journal of Petroleum Science and Engineering*, 45: 83– 96.

Chan, Y.T. and Banerjee, S. 1981. Analysis of Transient Three Dimensional Natural Convection in Porous Media. *J of Heat Transfer*, V – 103, May, 242 – 248.

Cheng, L. and Kuznetsov, A.V. 2005. Heat transfer in a laminar flow in a helical pipe filled with a fluid saturated porous medium", International Journal of Thermal Sciences 44, 787–798

Chu, C. 1983. Current In-Situ Combustion Technology. *J. Per. Tech.* August, 1412 – 1420.

Crookston, R.B., Culham, W.E. and Chen, W.H. 1979. A Numerical Simulation Model Recovery Processes for Thermal Recovery Processes. SPE Journal, February, 37 – 58.

Dawkrajai, P., Lake, L.W., Yoshioka, K., Zhu, D. and Hill, A.D. 2006. Detection of water or gas Entries in horizontal Wells from Temperature Profiles. presented at SPE/DOE symposium on improved oil Recovery, Tulsa, Oklahoma, USA, April 22-26, SPE – 100050.

Golczynski, T.S. and Niesen, V.G. 2004. Thermal Behavior During Restart of Ultradeepwater Flowlines. *SPE Production & Facilities*, May, 59 – 66.

Green, D.W. and Willhite, G.P. 1998. Enhanced oil Recovery. *SPE Textbook series*, vol. 6, Richardson, Texas, USA.

Hagoort, J. 2004. Ramey's Wellbore Heat Transmission Revisited," *SPE Journal*, December, 465 – 474 and SPE – 87305.

Hossain, M. E., Mousavizadegan, S. H. and Islam, M. R. 2008. The Effects of Thermal Alterations on Formation Permeability and Porosity. Petroleum Science and Technology, 26(10-11), pp. 1282 – 1302.

Hossain, M. E., Mousavizadegan, S. H. and Islam, M. R. 2007. Variation of Rock and Fluid Temperature during Thermal Operation in Porous Media. Petroleum Science and Technology, accepted for publication, article ID – 310718(PET/07/088), in press.

Jiang, P.X. and Lu, X.C. 2006. Numerical simulation of fluid flow and convection heat transfer in sintered porous plate channels. International Journal of Heat and Mass Transfer, 49, 1685–1695.

Kaviany, M. 2002. Principles of Heat Transfer. *John Wiley & Sons, Inc*., New York, USA, 885 – 897.

Kaye, S. E., Ting, V, C., and Fair, I, C. 1982. Development of a System to Utilize Flue Gas from Enhanced Oil Recovery Combustion Projects. *J. Per. Tech.* January, 181 – 88.

Khan, M.M., Prior, D., and Islam, M.R. 2005. Direct-Usage solar Refrigeration: From Irreversible Thermodynamics to Sustainable Engineering. presented in *Jordan International Chemical Engineering Conference*, V. 12-14 September, Amman, Jordan paper no - JICEC05-CHE-4-27.

Marx, J.W. and Langenheim, R.N. 1959. Reservoir heating by hot fluid injection", *Trans., AIME*, 216, 312.

Meyer, B.R, .1989. Heat Transfer in Hydraulic Fracturing. SPE Production Engineering, November, 423 – 429.

Yoshioka, K., Zhu, D., Hill, A.D., Dawkrajai, P. and Lake, L.W. 2005. A Comprehensive Model of Temperature Behavior in a Horizontal Well. SPE – 95656, presented at SPE Annual Technical Conference and Exhibition, Dallas, Texas, USA, October 09 – 12.